



OPEN

# Author Correction: Adrenergic inhibition facilitates normalization of extracellular potassium after cortical spreading depolarization

Hiromu Monai, Shinnosuke Koketsu, Yoshiaki Shinohara, Takatoshi Ueki, Peter Kusk, Natalie L. Hauglund, Andrew J. Samson, Maiken Nedergaard & Hajime Hirase

Correction to: *Scientific Reports* <https://doi.org/10.1038/s41598-021-87609-w>, published online 14 April 2021

The original version of this Article contained errors in Figure 3 (B) and (C), where grey shadings were incorrectly positioned.

The original Figure 3 and accompanying legend appear below.

The original Article has been corrected.

Published online: 18 March 2022

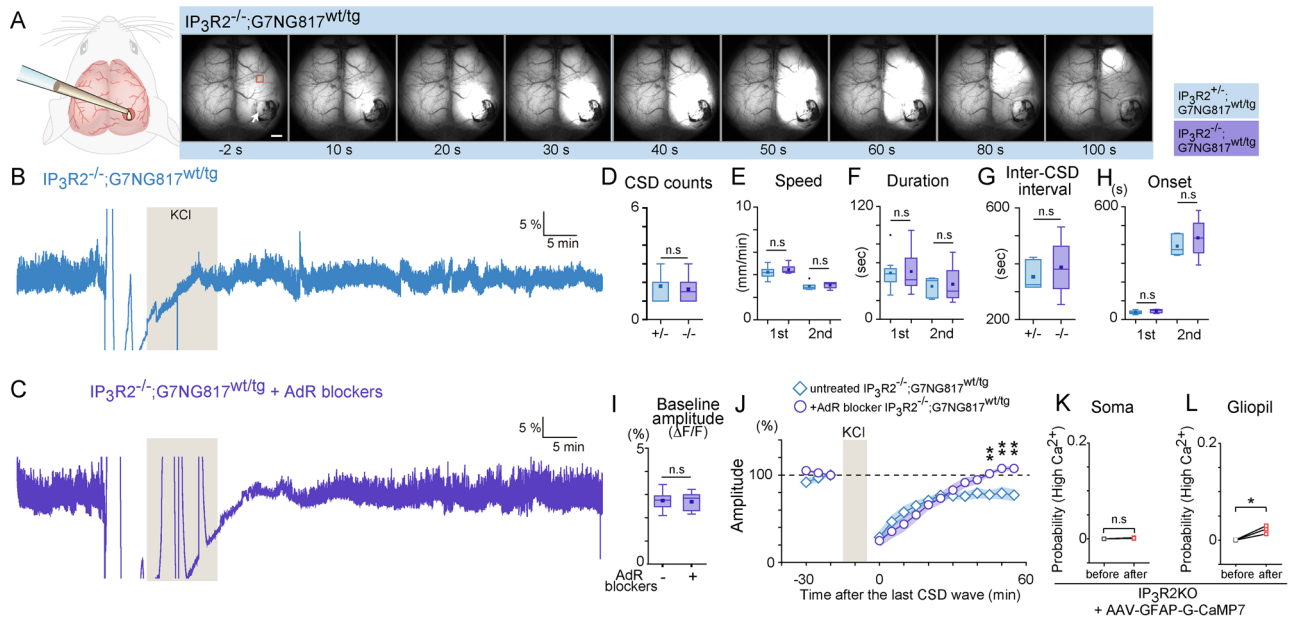


**Figure 3.** CSD propagation and neural activity recovery in  $IP_3R2$  KO mice. **(A)** Representative image of the time series of CSD propagation. Other than using  $IP_3R2^{-/-};G7NG817^{wt/tg}$  double transgenic mouse as subjects, the experimental conditions are the same as in Fig. 1. Scale bar 1 mm. **(B)** Example trace of  $Ca^{2+}$  activity of an ROI located  $\sim 2$  mm anterior to the KCl application site (Black square indicated in **A**). Note that neural activity does not recover completely within 50 min. **(C)** Similar  $Ca^{2+}$  signal trace as **(B)**, measured in an  $IP_3R2^{-/-};G7NG817^{wt/tg}$  mouse pretreated with AdR blockers. **(D)** Comparison of CSD  $Ca^{2+}$  wave number during 10 min KCl application between  $IP_3R2^{-/-};G7NG817^{wt/tg}$  and  $IP_3R2^{-/-};G7NG817^{wt/tg}$  mice.  $1.8 \pm 0.2$  vs.  $1.6 \pm 0.3$ , from  $N = 10$  vs.  $N = 8$ ,  $p = 0.64$ . **(E)** Comparison of CSD  $Ca^{2+}$  propagation speed between  $IP_3R2^{-/-};G7NG817^{wt/tg}$  and  $IP_3R2^{-/-};G7NG817^{wt/tg}$  mice. First wave:  $4.2 \pm 0.2$  vs.  $4.5 \pm 0.1$  mm/min; second wave:  $5.5 \pm 1.4$  vs.  $3.1 \pm 0.2$  mm/min. **(F)** Comparison of CSD  $Ca^{2+}$  wave duration between  $IP_3R2^{-/-};G7NG817^{wt/tg}$  and  $IP_3R2^{-/-};G7NG817^{wt/tg}$  mice. First wave:  $49.3 \pm 5.4$  vs.  $50.9 \pm 8.0$  s; second wave:  $35.0 \pm 3.8$  vs.  $37.4 \pm 11.6$  s. **(G)** Comparison of inter-CSD  $Ca^{2+}$  wave interval between  $IP_3R2^{-/-};G7NG817^{wt/tg}$  and  $IP_3R2^{-/-};G7NG817^{wt/tg}$  mice.  $353.5 \pm 20.9$  s vs.  $386.6 \pm 57.1$  s,  $N = 6$  vs.  $N = 4$ ,  $p = 0.54$ . **(H)** Comparison of first and second CSD  $Ca^{2+}$  wave onset time between  $IP_3R2^{-/-};G7NG817^{wt/tg}$  (WT, black) and  $IP_3R2^{-/-};G7NG817^{wt/tg}$  ( $IP_3R2$  KO, blue) mice. First wave:  $38.3 \pm 2.6$  vs.  $45.0 \pm 3.2$  s,  $N = 10$  vs.  $N = 8$ ; second wave:  $391.4 \pm 22.1$  vs.  $434.3 \pm 59.5$  s,  $N = 7$  vs.  $N = 4$ . **(I)** Comparison of baseline amplitude before AdR blocker in  $IP_3R2^{-/-};G7NG817^{wt/tg}$  mice. **(J)** Effect of AdR blocker pretreatment on the recovery of neural oscillations after KCl-induced CSD in  $IP_3R2^{-/-};G7NG817^{wt/tg}$  mice. Recovery is facilitated by AdR blocker pretreatment ( $N = 6$ ) compared with the untreated control group ( $N = 6$ ). **(K, L)** Comparisons of mean somatic and gliopil  $Ca^{2+}$  probability in  $IP_3R2$  KO expressing G-CaMP7 in astrocytes via AAV (**I**, 80 cells vs. 113 cells from  $N = 3$  mice) and gliopil  $Ca^{2+}$  events in  $IP_3R2$  KO mice (**J**,  $N = 3$  mice). \* $p < 0.05$ .



**Open Access** This article is licensed under a Creative Commons Attribution 4.0 International License, which permits use, sharing, adaptation, distribution and reproduction in any medium or format, as long as you give appropriate credit to the original author(s) and the source, provide a link to the Creative Commons licence, and indicate if changes were made. The images or other third party material in this article are included in the article's Creative Commons licence, unless indicated otherwise in a credit line to the material. If material is not included in the article's Creative Commons licence and your intended use is not permitted by statutory regulation or exceeds the permitted use, you will need to obtain permission directly from the copyright holder. To view a copy of this licence, visit <http://creativecommons.org/licenses/by/4.0/>.

© The Author(s) 2022